

# Wintertime blocking regimes over Europe are projected to become less persistent in a warming climate

Joshua Dorrington<sup>1</sup>, Kristian Strommen<sup>2</sup>, Federico Fabiano<sup>3</sup>, and Franco Molteni<sup>4</sup>

<sup>1</sup>Karlsruhe Institute of Technology

<sup>2</sup>University of Oxford

<sup>3</sup>CNR

<sup>4</sup>European Centre for Medium-Range Weather Forecasts

November 23, 2022

## Abstract

To better understand the impacts of climate change on Europe, it is important to understand changes in the wintertime large-scale circulation. The framework of weather regimes provides a powerful tool for studying the highly nonlinear Euro-Atlantic circulation, but exactly how these regimes will be altered by anthropogenic climate change is still imperfectly understood. Using the recently developed approach of geopotential-jet regimes, applied to an ensemble of state-of-the-art CMIP6 models, we show that the centres of action of anticyclonic regimes are not projected to change substantially by the end of century, even under an extreme warming scenario. Instead, the regimes are expected to become less persistent, making long-lived blocking events less likely. We show that these two key elements of the regime response can be captured in a simple Lorenz-like model subjected to parameter variations, emphasising the conceptual link between observed atmospheric regimes and the regimes identified in basic mathematical systems.

1 **Wintertime blocking regimes over Europe are projected**  
2 **to become less persistent in a warming climate**

3 **Josh Dorrington<sup>1,2</sup>, Kristian Strommen<sup>1</sup>, Federico Fabiano<sup>3</sup>, Franco Molteni<sup>4</sup>**

4 [1  
5 ]Atmospheric, Oceanic, and Planetary Physics, University of Oxford, Oxford, UK

6 [2  
7 ]Institute for Meteorology and Climate (IMK-TRO), Karlsruhe Institute of Tech-  
8 nology, Germany

9 [3  
10 ]Institute of Atmospheric Sciences and Climate (ISAC-CNR), Bologna, Italy

11 <sup>4</sup>European Centre for Medium Range Weather Forecasting, Shinfield Road, Reading, UK

12 **Key Points:**

- 13 • The spatial structure of anticyclonic circulations over Europe are projected to stay  
14 the same under climate change.  
15 • The persistence of these anticyclonic circulations are in general expected to de-  
16 crease, although there is considerable inter-model variability  
17 • We show that these qualitative features of the atmospheric response can be repro-  
18 duced in a simple forced regime model.

---

Corresponding author: Joshua Dorrington, [joshua.dorrington@kit.edu](mailto:joshua.dorrington@kit.edu)

## Abstract

In order to better understand the impacts of climate change on Europe, it is important to understand changes in the wintertime large-scale circulation. The framework of weather regimes provides a powerful tool for studying the highly nonlinear Euro-Atlantic circulation, but exactly how these regimes will be altered by anthropogenic climate change is still imperfectly understood. Using the recently developed approach of geopotential-jet regimes, applied to an ensemble of state-of-the-art CMIP6 models, we show that the centres of action of anticyclonic regimes are not projected to change substantially by the end of century, even under an extreme warming scenario. Instead, the regimes are expected to become less persistent, making long-lived blocking events less likely. We show that these two key elements of the regime response can be captured in a simple Lorenz-like model subjected to parameter variations, emphasising the conceptual link between observed atmospheric regimes and the regimes identified in basic mathematical systems.

## Plain language summary

The impact of climate change on European weather can be broken into two components: a thermodynamic part relating to increasing air temperature and humidity, and a dynamic part relating to changes in the atmospheric circulation such as the direction and strength of prevailing winds. While the thermodynamic part is relatively well understood, the dynamic part is very uncertain and this is a major problem in constraining European climate projections.

Looking at the winter season, we study the dynamic response of CMIP6 models under climate change using so-called 'regimes', and show that the types of prevailing circulation are not predicted to change strongly. However the regimes are projected to be less long lived.

We also show that these features can be well captured in a simple 5 equation model of regime dynamics, providing a potentially useful tool for understanding regime systems in more detail.

## 1 Introduction

How will anthropogenic climate change impact Europe? The socio-economic risks associated with extreme weather are likely to intensify over the 21st century (Forzieri et al., 2016), and the large-scale trend is towards warmer conditions with more intense rainfall (Coppola et al., 2021), as a result of reasonably well-understood thermodynamic changes. However, on a regional level, uncertain dynamical changes in the circulation can substantially modify and even reverse this trend. As one example, the CMIP6 ensemble shows a *drying* trend over the Mediterranean (Zappa & Shepherd, 2017), driven by models which predict a strengthening of the polar vortex and tropical amplification under climate change. Uncertainties in the dynamical response of the circulation are thus a major barrier towards developing a more detailed picture of regional climate trends (Shepherd, 2014; Vallis et al., 2015; Shepherd, 2019). The Euro-Atlantic circulation is particularly complex during Boreal winter, due to the highly nonlinear dynamics associated with persistent blocking (Davini & D'Andrea, 2016; Schiemann et al., 2020), latitudinal 'wobbling' of the jet stream (T. Woollings et al., 2010; Parker et al., 2019) and Rossby wave breaking (T. J. Woollings et al., 2008; Masato et al., 2012), all of which are common during the DJF season.

The concept of weather regimes provides a useful framework for understanding this flow by discretising the continuous atmospheric state into a small number of qualitatively distinct flow patterns. Euro-Atlantic regimes are commonly studied either from the perspective of circulation regimes found in the geopotential height field (Michelangeli et al.,

1995; Grams et al., 2017; Fabiano et al., 2020) or from a jet regime perspective, based on the trimodal distribution of the low level jet stream (Hannachi et al., 2012; Madonna et al., 2017). Regimes have been used to characterise the flow-dependent predictability (Ferranti et al., 2015) and surface impacts of synoptic weather (Grams et al., 2017; van der Wiel et al., 2019), the impact of remote teleconnections on Europe (Cassou, 2008), and, recently, forced climate trends (Fabiano et al., 2021).

Much of the uncertainty in the wintertime dynamical response to climate change can be framed as uncertainty in the forced response of these regimes. It has been suggested (Palmer, 1993, 1999), using insights drawn from the conceptual Lorenz '63 model (Lorenz, 1963), that the first-order response of regimes to climate forcing will be to change their 'temporal' behaviour – altering the occurrence probabilities of the different regimes – while leaving the 'spatial' characteristics of the regimes – that is, their positions in phase space – largely unaltered. Put another way, climate forcing may manifest as certain historically-present weather patterns becoming more or less probable, but without the emergence of completely new preferred weather patterns. Despite the importance of understanding Euro-Atlantic regime behaviour, this hypothesis has never been tested in climate models. This is at least in part due to the considerable sampling variability in many regime methodologies, and severe deficiencies in regime representation in previous generations of climate models that would make such an analysis unreliable. To avoid such issues, many regime studies assume a set of fixed reference patterns, rendering it impossible to consider the role of spatial regime variability.

Recently, a hybrid approach to regime identification has been introduced (Dorrington & Strommen, 2020; Dorrington et al., 2022), termed geopotential-jet regimes, that integrates both jet speed and geopotential height data. Guided by the observation that the predominantly linear variability of the eddy-driven jet stream is uncorrelated to the non-linear variations of the jet latitude (Parker et al., 2019), variability in 500hPa geopotential height is decomposed into a linearly varying component reflecting meridional gradients induced by jet speed variability, and a nonlinear component that emphasises the multimodal regime dynamics, and jet stream deviations. Geopotential-jet regimes are then identified in this non-linear residual space. As atmospheric blocking events are closely tied to deviations of the jet stream, this approach focuses on anticyclonic regimes rather than cyclonic and zonally symmetric states. Conceptually, This asymmetry is conceptually well-justified, as it is blocking flows which are most strongly associated with highly non-linear dynamics.

In Dorrington et al. (2022), a set of three geopotential-jet regimes were found to be particularly robust to observational sampling variability in a number of reanalyses, and were also well captured by most CMIP6 models in the historical period. Both robustness and a reasonable historical fidelity in models are necessary features for an analysis of a regime's forced dynamics to be trustworthy. Therefore in this work, we are able to test the holistic nature of the Euro-Atlantic regime response, both spatial and temporal, for the first time, building on prior analyses of regimes' temporal response to climate change such as in Fabiano et al. (2021). Specifically, we analyse changes in regime structure in twenty CMIP6 models (detailed in supplementary table 1) under the SSP5-8.5 climate change scenario. This scenario has been characterised as relatively unlikely and represents an extreme future rather than a baseline 'best guess' emissions scenario (Burgess et al., 2020). However as circulation regime occurrence and persistence has been found to vary approximately linearly with increasing warming (Fabiano et al., 2021), we consider only this most extreme scenario here in order to obtain the clearest dynamical signal possible.

## 116 2 Methods

### 117 2.1 CMIP6 Data

118 We analyse simulations from the 6th phase of the coupled model inter-comparison  
 119 project (CMIP6), analysing the twenty model simulations listed in supplementary ta-  
 120 ble 1. We consider both historical experiments, which consist of coupled uninitialised cli-  
 121 mate runs forced with historical greenhouse gas and aerosol forcings over the 20th cen-  
 122 tury, and future climate projections produced under the SSP5-8.5 climate change sce-  
 123 nario.

### 124 2.2 Regime methodology and metrics

125 A single time series of daily DJF Z500 anomalies over the region [80W-40E,30N-  
 126 90N] was created for each model by appending historical and SSP5-8.5 simulations, and  
 127 detrended using a cubic fit to the area-averaged Z500 field over the same region. The  
 128 four leading principal components of detrended Z500 were then computed. A correspond-  
 129 ing jet speed time series was also computed, defined as the maximum (oriented Eastward)  
 130 of 5-day smoothed latitudinally averaged 850 hPa zonal wind speed over the Atlantic do-  
 131 main [100W-80E, 30-90N]. The fraction of principal component variability explicable by  
 132 linear variations in the jet speed were identified for each model via linear regression, and  
 133 the space of residuals to this linear best fit was used to identify regimes via K-means clus-  
 134 tering. For a more in depth explanation of the method, and expanded motivation, see  
 135 Dorrington & Strommen (2020) and Dorrington et al. (2022). Jet speed was not detrended,  
 136 as trends were found to be insignificant, but the linear relationship between principal com-  
 137 ponents and jet speed was calculated separately for the historical and future time pe-  
 138 riods. After regimes had been identified using K-means, each day in each dataset was  
 139 assigned to the regime it lay closest to in the residual phase space, unless the pattern  
 140 correlation of the Z500 anomaly field for that day with the regime Z500 composite (see  
 141 figure 1) was less than 0.4, in which case it was labelled as a Neutral state.

142 Regime occurrence is defined as the fraction of days belonging to a given regime,  
 143 while regime persistence is defined as the probability that a regime event persists from  
 144 one day to the next, and is found by fitting a Markov chain to the daily sequence of regimes.

### 145 2.3 Regime reconstruction

146 Figures 1d) and e) show area-weighted pattern correlations between Z500 anomaly  
 147 fields and reconstructed fields computed from the regime time series. Daily reconstruc-  
 148 tions were obtained by simply using the regime anomaly composite assigned to a given  
 149 day. Seasonal reconstructions were found by first computing the occurrence fraction of  
 150 each regime over a given season, and then using an occurrence-weighted sum of the regime  
 151 anomaly composites as the reconstructed seasonal pattern.

### 152 2.4 Molteni Kucharski model

153 The Molteni Kucharski model is a 5-equation system of ordinary differential equa-  
 154 tions, which provides a heuristic model of bimodality in the Euro-Atlantic, as driven by  
 155 the interaction of heat fluxes with climatological standing waves. It therefore provides  
 156 a natural low-dimensional analogue of the multimodal regimes found in observations and  
 157 complex models. Its form is given by:

$$\begin{aligned}
 \frac{\partial U_{\text{th}}}{\partial t} &= \sigma(A - U_{\text{btr}}) + (\gamma - \sigma)A - \kappa U_{\text{th}} - c_a(E^2 - E_0^2) \\
 \frac{\partial A}{\partial t} &= U([B^* - \sigma] - B') - \kappa A \\
 \frac{\partial B'}{\partial t} &= UA - \kappa B' \\
 \frac{\partial U_{\text{btr}}}{\partial t} &= -\kappa_f U_{\text{btr}} + c_f(E^2 - E_0^2) \\
 \frac{\partial E}{\partial t} &= -\tilde{\kappa}_E E + (c_a U_{\text{th}} - c_k U_{\text{btr}})E
 \end{aligned}$$

158 where  $U_{\text{btr}}$  and  $U_{\text{th}}$  are barotropic and thermally-driven zonal wind speed anom-  
 159 lies over the Euro-Atlantic respectively,  $A$  and  $B$  are amplitudes of sinusoidal stream-  
 160 function modes over the Euro-Atlantic, in and out of phase with the NAO respectively,  
 161  $E$  is a basin wide eddy amplitude, and:

$$\tilde{\kappa}_E = \kappa_f \left[ \sqrt{1 + \frac{E^2}{E_0^2}} - \sqrt{2} \right] \quad (1)$$

$$U = U_{\text{th}} + U_{\text{btr}} \quad (2)$$

162 The  $B^*$  parameter approximately represents the climatological forcing of the land-  
 163 sea temperature contrast, and we use changes in this parameter to approximate the im-  
 164 pacts of climate change on the system. Other non-varying parameters are described in  
 165 detail in Molteni & Kucharski (2019). For each parameter value, the model is integrated  
 166 using a Runge-Kutta fourth-order scheme for 2000,000 model time units. Two regimes  
 167 were identified based on the sign of the  $U$  variable.

### 168 3 Results

#### 169 3.1 CMIP6

170 Figure 1a) shows the 500 hPa geopotential height (Z500) anomaly associated with  
 171 each of the three geopotential-jet regimes, averaged across the twenty CMIP6 models for  
 172 DJF daily data in the historical period 1950-2010. The Atlantic ridge (AR), Negative  
 173 NAO (NAO-) and Blocking (BLK) patterns are associated with anticyclonic anomalies  
 174 over the Eastern Atlantic, Greenland and Scandinavia respectively, and capture the main  
 175 deviations from a zonally symmetric flow seen in the Euro-Atlantic region. Figure 1b)  
 176 shows equivalent regime anomalies, but now calculated under the future warming sce-  
 177 nario SSP5-8.5, for the period 2070-2100. By eye, the end-of-century patterns are almost  
 178 indistinguishable from those identified in the historical period: it is only by reference to  
 179 1c), which shows the difference between b) and a), that changes in the anomalies can be  
 180 seen. The NAO- regime features a weakened meridional dipole in the SSP5-8.5 simula-  
 181 tions, and has its geopotential low shifted further east. The AR regime likewise features  
 182 a slightly weakened dipole and a very minor eastward shift of the ridge. The BLK regime  
 183 is largely unchanged but features a slight strengthening of its zonally oriented dipole.  
 184 These changes, while in places significant at the 5% level according to a bootstrap test,  
 185 are minor, and are at all gridpoints less than 25% of the amplitude of the circulation anom-  
 186 alies themselves, representing a slight modulation of pattern amplitude but with few changes  
 187 in the shape of the pattern. We can quantify the importance these small spatial regime  
 188 changes have on the evolution of the Z500 field, by attempting to reconstruct the Z500

189 field using the three regime anomalies and assessing the average pattern correlation be-  
 190 tween the full and reconstructed fields. We do this over the period 2070-2100 using both  
 191 historical and future regime anomalies. If the nature of the flow is strongly altered in  
 192 the future climate then the ability of historical regime patterns to characterise future Z500  
 193 variability will be reduced. In fact however, on both daily (figure 1d)) and seasonal timescales  
 194 (1e), there is no substantial difference in the ability of regimes to explain Z500 variabil-  
 195 ity, as assessed via the pattern correlation, when comparing historical and future regime  
 196 patterns. This strongly supports then the hypothesis of Palmer (1999) that the impact  
 197 of external forcing on regime patterns is negligible and can be ignored.

198 Moving on to the temporal variability, figure 2 shows the CMIP6 ensemble mean  
 199 occurrence and persistence anomalies, with a confidence interval estimated using a drop-  
 200 1 bootstrap approach. Trends in regime occurrence are quite weak for the AR and BLK  
 201 regimes, in both cases less than 1% shifts over a 100-year period, and there is no trend  
 202 in NAO- occurrence. This differs from the findings using classical circulation regimes of  
 203 Fabiano et al. (2021). There, clear trends in regime occurrence were found, especially  
 204 for the NAO+ regime. It is likely that methodological differences, namely the inclusion  
 205 of a neutral state, and a focus on anticyclonic regimes which explains this difference. In  
 206 our approach regime persistence shows a pronounced signal, with all regimes showing  
 207 a trend towards reduced regime lifetimes. The signal is strongest for the AR and BLK  
 208 regimes, which show reductions in the probability of persistence of 2.4% and 2.3% re-  
 209 spectively, and a near-linear decrease over time. The NAO- regime also shows a robust  
 210 decrease in regime persistence, although not as strongly, with a 1.5% decrease in per-  
 211 sistence probability over the century, associated with a sharp drop-off after the period  
 212 2000-2060. These trends are not large compared to the interannual and even interdecadal  
 213 regime variability seen in the historical record (Dorrington et al., 2022), but still repre-  
 214 sent significant shifts, equivalent to the magnitude of historical model bias for some regimes.  
 215 That persistence trends are most

216 The ensemble mean trends do however obscure considerable inter-model variabil-  
 217 ity, as shown in figure 3 for persistence (inter-model variability in occurrence is shown  
 218 in supplementary figure 1). For all regimes, there is no clear model consensus on the sign  
 219 of climate trends. Models are most confident in the reduced persistence of the AR regime,  
 220 with 75% of models agreeing. The trend in NAO- regime persistence is particularly un-  
 221 certain, with the mean response skewed by a small number of models experiencing per-  
 222 sistence drops exceeding 10%. It is worth noting that the two most extreme outliers in  
 223 NAO- persistence are models from the same centre, the Met Office UKESM1-0-LL and  
 224 HadGEM3-GC31-LL models, and so can not be considered independent of each other.  
 225 The same effect can be seen to a much lesser degree in the plume of BLK persistence trends,  
 226 with a few models projecting particularly strong decreases in persistence. The BLK and  
 227 NAO- persistence trends are linked, as models which project decreased BLK persistence  
 228 also tend to project decreased NAO- persistence (not shown).

### 229 3.2 Molteni-Kucharski model

230 We have shown that the hypothesis, first inspired by experiments in the Lorenz '63  
 231 model, that climate change would leave regime patterns largely unchanged is in agree-  
 232 ment with the CMIP6 projections, even under the most extreme climate scenarios. How-  
 233 ever while Palmer (1999) suggested the climate change signal would project primarily  
 234 on changes in regime occurrence, here we have found persistence to be most affected.

235 To address this issue, we look at the Molteni-Kucharski (MK) model (Molteni &  
 236 Kucharski, 2019) which can be considered as a generalisation of Lorenz '63, coupled to  
 237 a nonlinear oscillator. It provides a heuristic model of the dynamics of the North Atlantic  
 238 Oscillation, constructed from a truncation of barotropic dynamics over the Euro-Atlantic

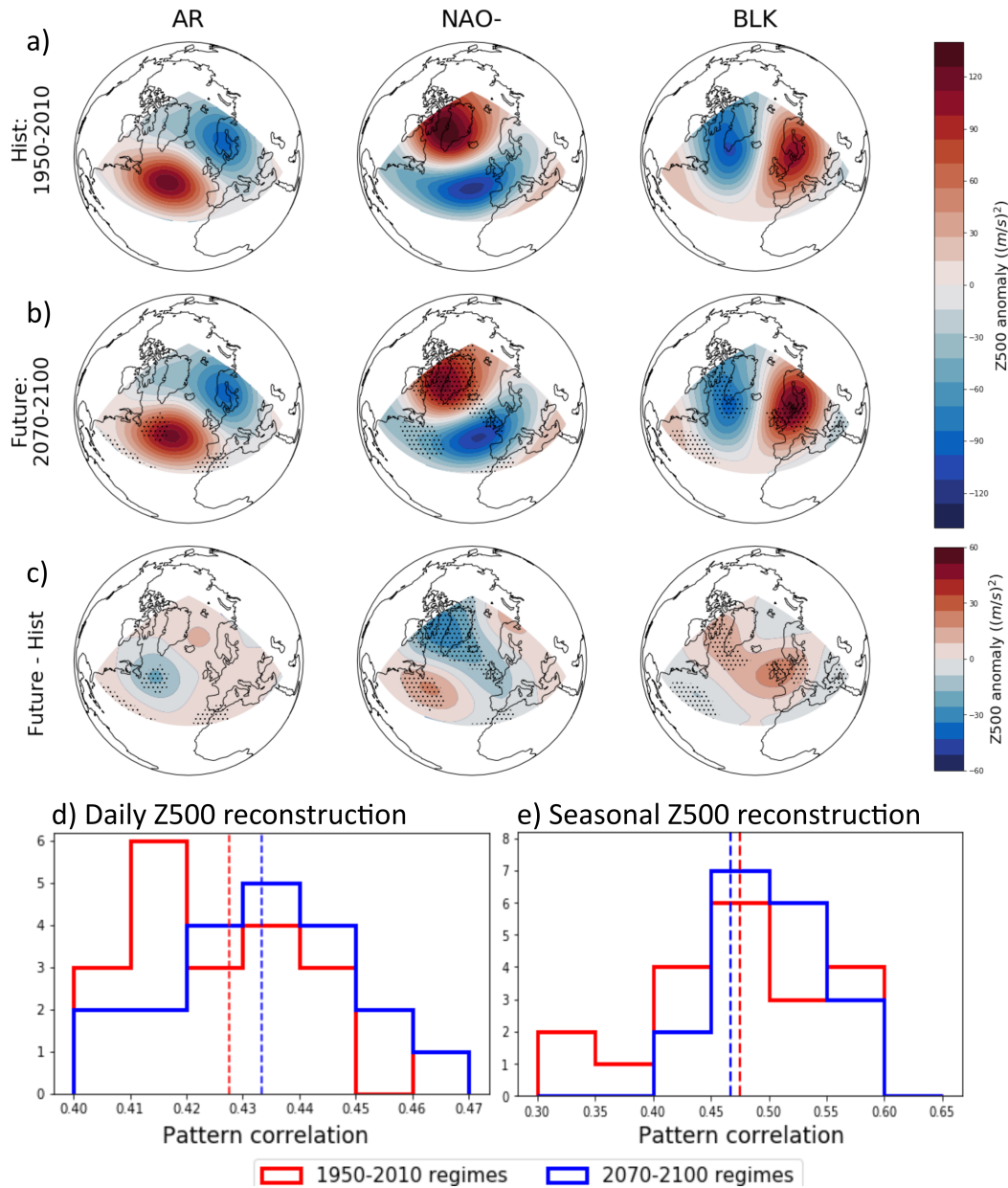


Figure 1: a) Composites of seasonally detrended Z500 anomalies, averaged across all DJF days assigned to a given regime in the period 1950-2010, averaged across the twenty CMIP6 models. b) As a) but for the period 2070-2100, computed using the SSP5-8.5 simulations. Stippling indicates gridpoints where anomalies are different from a) at the 95% level, estimated using a bootstrap approach. c) The difference between b) and a). Stippling as in b). d) A histogram over the twenty CMIP6 models showing the average pattern correlation between the regime assigned to each day in DJF 2070-2100, and the full Z500 anomaly field. Correlations found with historical regime patterns are shown in red, and correlations found with future regime patterns in blue. Dashed vertical lines show the ensemble mean value. e) as d), but for correlations of seasonal DJF anomalies, where the regime reconstruction has been computed from a weighted sum of regime patterns, based on their seasonal occurrence probability.

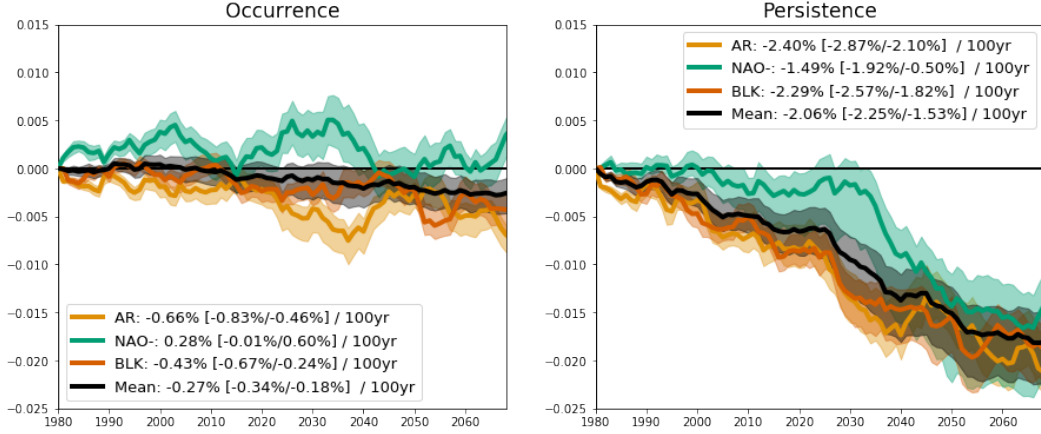


Figure 2: 60-year rolling windows of CMIP6 ensemble mean regime occurrence and persistence anomalies relative to 1950-2010, with the date along the x-axis indicating the central year of the window. Shading indicates a confidence interval in the ensemble mean estimated from a drop-1 bootstrap approach.

239 region, with a free wave mode interacting with a standing wave generated by climato-  
 240 logical ocean heat fluxes and meridional and zonal temperature gradients.

241 We introduce an analog of climate change into the MK model by altering the  $B^*$   
 242 parameter, which can be broadly understood as representing changes in the climatolog-  
 243 ical wave mode, consistent with changes in the land-sea contrast anticipated under cli-  
 244 mate change (Joshi et al., 2008; Dong et al., 2009). However it should be emphasised that  
 245 the simplicity of the MK model hinders a literal interpretation of individual parameters,  
 246 and so the model should be understood as a conceptual analog of a forced regime sys-  
 247 tem, rather than representing a direct simplification of the regime dynamics seen in  
 248 seen in the CMIP6 ensemble.

249 Figure 4 shows integrations of the MK model subject to variations of  $B^*$  across the  
 250 range  $B^* = [11 - 17]$ . The system possesses a bimodal regime behaviour, which can  
 251 be understood as a transition between a zonally symmetric state and a blocked state.  
 252 As  $B^*$  increases, the duration of the regime events decrease. Figure 5a) shows that changes  
 253 in the mean state of the 5 variables, conditioned on regime, are negligible; just as we see  
 254 in CMIP6, the impact of forcing does not strongly impact the regime patterns. Regime  
 255 occurrence (figure 5b)) shows no consistent linear trend across the parameter range, but  
 256 deviations towards more asymmetrical regime are seen, with occurrence shifts exceed-  
 257 ing 5% for  $B^* \approx 15 - 16$ , a result not clearly in the CMIP6 ensemble.

258 Trends in regime persistence however are larger, predominately linear and asym-  
 259 metrical between the regimes, with decreased persistence of 8%-10% between  $B^* = 11$   
 260 and  $B^* = 17$ . While of course such a simple model can not capture many of the sub-  
 261 tleties seen in the CMIP6 ensemble, the fact that we obtain a qualitative agreement with  
 262 the CMIP6 forced regime behaviour demonstrates the sometimes surprising efficacy of  
 263 low-dimensional models for describing complex physical phenomena.

264 **4 Discussion**

265 In this paper we have characterised the forced response of anticyclonic weather regimes  
 266 – which play a key role in the wintertime Euro-Atlantic circulation – under climate change  
 267 within the CMIP6 ensemble. We show for the first time that regime patterns are pro-

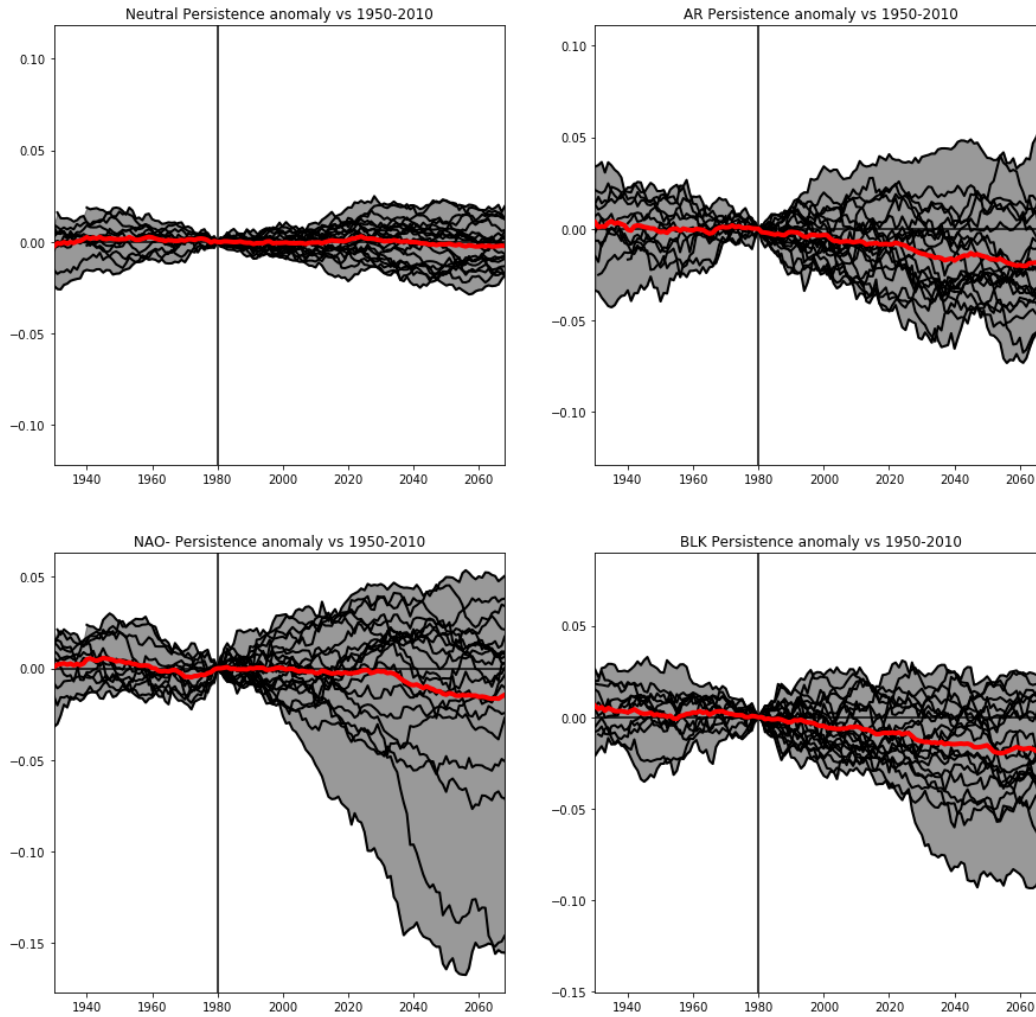


Figure 3: Sixty year rolling windows of regime occurrence anomaly, with each CMIP6 model shown in black, and with the ensemble mean (as in figure 2) in red. The vertical line marks the reference period of 1950-2010. Shading tracks the full range of intermodel spread as a visual guide.

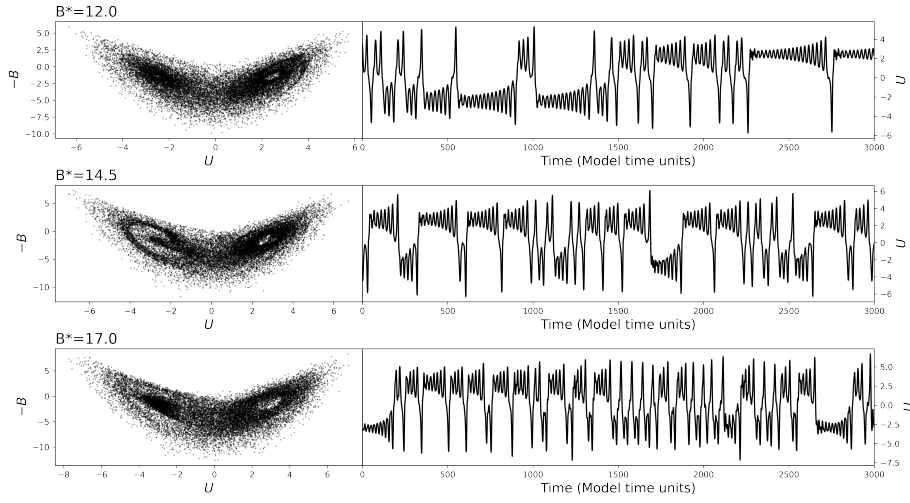


Figure 4: Left: Integrations of the MK model, showing the bimodality of the  $U$ - $B$  subspace (equivalent to the  $x$ - $z$  subspace in the L63 model), for a range of considered  $B^*$  values. Right: Corresponding 3000 MTU time series of the  $U$  showing changes in average regime lifetime as  $B^*$  increases.

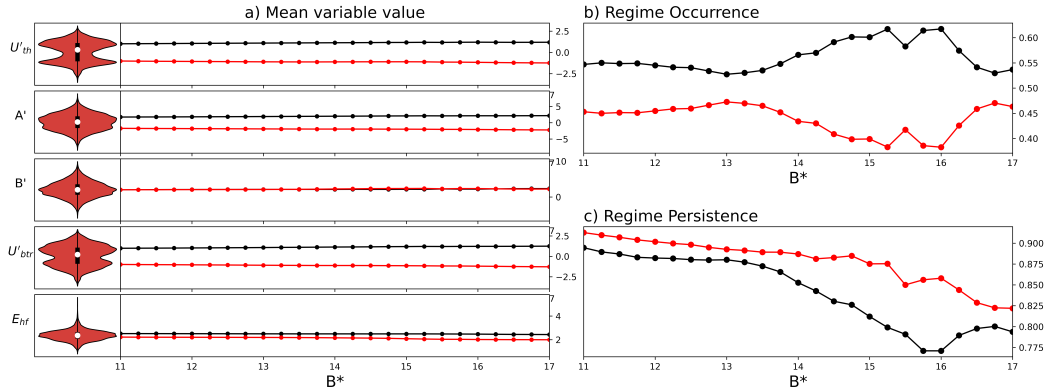


Figure 5: a) Violin plots show probability distributions of the 5 variables in the KM model for the standard parameter value  $B^*=12$ . Black and red dotted lines show the average values of each of those variables in the two regimes for increasing values of  $B^*$ . b) Changes in regime occurrence as a function of increasing  $B^*$ . c) as in b) but showing regime persistence changes.

jected to remain largely unaltered in a warming climate, suggesting that the position of ridges and persistent blocks in the Euro-Atlantic region is unlikely to alter. As such anticyclonic features are a main driver of wintertime cold extremes and flooding in Europe, this stationarity in patterns places constraints on regional climate changes. We found regime occurrence probabilities largely unaltered in a warming climate, with the dominant impact being a decrease in the persistence of all regimes. Intermodel uncertainty however is large, and there is no model consensus on even the sign of persistence change for the BLK and NAO- regimes.

We showed that the qualitative properties of the CMIP6 regime response – stationary regime patterns with decreasing persistence – can be reproduced in a forced 5-equation conceptual regime model. We therefore answer a long-standing hypothesis on the dynamics of forced regime systems, as well as highlighting the value of simple models for understanding even high-dimensional multi-scale flows. The decrease in regime persistence we document – and the corresponding weak decrease in the total fraction of days featuring anticyclonic blocking regimes – is consistent with previous work finding less intense and less frequent blocking events (Masato et al., 2013, 2014; Rousi et al., 2021; Fabiano et al., 2021). Although there is not a clear consensus on this trend, with some reports of insignificant projected changes in blocking (Bacer et al., 2021), our results lend weight to the majority view of less anticyclonic blocking. This is also consistent with emerging evidence for a more zonal future circulation, and a latitudinal squeezing of the jet (Barnes & Polvani, 2013a; Peings et al., 2017).

This increased zonalisation will tend to result in wetter, more mild winters for Western Europe, with an associated drying trend for north-west Africa and southern Europe, as a result of fewer southern excursions of the low-level jet (Driouech et al., 2010). However, the trends we observe in regime persistence are small compared to interdecadal variability even under the most extreme SSP5:8.5 scenario, as has been seen in other aspects of the Euro-Atlantic circulation (Barnes & Polvani, 2013b; Blackport & Screen, 2020). The implication is that, in the short term and under desirable low-emission scenarios, interdecadal forecasts capturing both forced and internal variability of the Earth system provide the best avenue for understanding 21st century Euro-Atlantic climate. This is especially the case in light of recent results showing decadal forecast skill in both the NAO (Smith et al., 2020) and Euro-Atlantic blocking dynamics (Athanasiadis et al., 2020). One possible risk of decreased regime persistence is an increased number of regime transitions, which are challenging to predict reliably and so could plausibly decrease Euro-Atlantic predictability. However, as NAO- conditions are associated with high predictability on both subseasonal and seasonal timescales (Weisheimer et al., 2017) while the BLK regime is linked to large forecast errors (Faranda et al., 2017; Büeler et al., 2021), it is not possible to comment confidently on likely predictability trends given the large intermodel spread in regime-specific trends.

## 5 Open Research

Raw CMIP6 data is available from:

<https://esgf-index1.ceda.ac.uk/search/cmip6-ceda/>

Processed regime data is available from:

[https://github.com/joshdorrington/CMIP6\\_future\\_regime\\_changes](https://github.com/joshdorrington/CMIP6_future_regime_changes)

## Acknowledgments

J. D. was funded by NERC as part of the Environmental Research Doctoral Training Program (Grant number NE/L002612/1). K. J. S. was funded by a Thomas Philips and

315 Jocelyn Keene Junior Research Fellowship in Climate Science at Jesus College, Oxford.  
 316 Federico Fabiano was funded by the European Commission’s Horizon 2020 research pro-  
 317 gramme (PRIMAVERA, grant no. 641727).

318 We acknowledge the World Climate Research Programme, which, through its Work-  
 319 ing Group on Coupled Modelling, coordinated and promoted CMIP6 and CMIP5. We  
 320 thank the climate modelling groups for producing and making available their model out-  
 321 put, the Earth System Grid Federation (ESGF) for archiving the data and providing ac-  
 322 cess, and the multiple funding agencies who support CMIP6, CMIP5, and ESGF.

## 323 References

- 324 Athanasiadis, P. J., Yeager, S., Kwon, Y.-O., Bellucci, A., Smith, D. W., &  
 325 Tibaldi, S. (2020, jun). Decadal predictability of North Atlantic blocking and  
 326 the NAO. *npj Climate and Atmospheric Science* 2020 3:1, 3(1), 1–10. Re-  
 327 trieved from <https://www.nature.com/articles/s41612-020-0120-6> doi:  
 328 10.1038/s41612-020-0120-6
- 329 Bacer, S., Jomaa, F., Beaumet, J., Gallée, H., Le Bouëdec, E., Ménégos, M.,  
 330 & Staquet, C. (2021). Impact of climate change on wintertime European  
 331 atmospheric blocking. *Weather and Climate Dynamics*. Retrieved from  
 332 <https://doi.org/10.5194/wcd-2021-47> doi: 10.5194/wcd-2021-47
- 333 Barnes, E. A., & Polvani, L. (2013a, sep). Response of the Midlatitude Jets, and of  
 334 Their Variability, to Increased Greenhouse Gases in the CMIP5 Models. *Journal*  
 335 *of Climate*, 26(18), 7117–7135. Retrieved from [https://journals.ametsoc.org/](https://journals.ametsoc.org/view/journals/clim/26/18/jcli-d-12-00536.1.xml)  
 336 [view/journals/clim/26/18/jcli-d-12-00536.1.xml](https://journals/clim/26/18/jcli-d-12-00536.1.xml) doi: 10.1175/JCLI-D-12-  
 337 -00536.1
- 338 Barnes, E. A., & Polvani, L. (2013b, sep). Response of the Midlatitude Jets, and of  
 339 Their Variability, to Increased Greenhouse Gases in the CMIP5 Models. *Journal*  
 340 *of Climate*, 26(18), 7117–7135. Retrieved from [https://journals.ametsoc.org/](https://journals.ametsoc.org/view/journals/clim/26/18/jcli-d-12-00536.1.xml)  
 341 [view/journals/clim/26/18/jcli-d-12-00536.1.xml](https://journals/clim/26/18/jcli-d-12-00536.1.xml) doi: 10.1175/JCLI-D-12-  
 342 -00536.1
- 343 Blackport, R., & Screen, J. A. (2020, feb). Insignificant effect of Arctic amplifi-  
 344 cation on the amplitude of midlatitude atmospheric waves. *Science Advances*(8),  
 345 eaay2880. doi: 10.1126/sciadv.aay2880
- 346 Büeler, D., Ferranti, L., Magnusson, L., Quinting, J. F., & Grams, C. M. (2021,  
 347 oct). Year-round sub-seasonal forecast skill for Atlantic–European weather  
 348 regimes. *Quarterly Journal of the Royal Meteorological Society*, 147(741), 4283–  
 349 4309. doi: 10.1002/QJ.4178
- 350 Burgess, M. G., Ritchie, J., Shapland, J., & Pielke, R. (2020, dec). IPCC baseline  
 351 scenarios have over-projected CO2 emissions and economic growth. *Environmental*  
 352 *Research Letters*, 16(1), 014016. doi: 10.1088/1748-9326/ABCDD2
- 353 Cassou, C. (2008). Intraseasonal interaction between the Madden-Julian Oscillation  
 354 and the North Atlantic Oscillation. *Nature*, 455(7212), 523–527. doi: 10.1038/  
 355 nature07286
- 356 Coppola, E., Nogherotto, R., Ciarlo’, J. M., Giorgi, F., van Meijgaard, E., Kadyrov,  
 357 N., ... Wulfmeyer, V. (2021, feb). Assessment of the European Climate Projec-  
 358 tions as Simulated by the Large EURO-CORDEX Regional and Global Climate  
 359 Model Ensemble. *Journal of Geophysical Research: Atmospheres*, 126(4). doi:  
 360 10.1029/2019JD032356
- 361 Davini, P., & D’Andrea, F. (2016, dec). Northern Hemisphere atmospheric block-  
 362 ing representation in global climate models: Twenty years of improvements? *Jour-  
 363 nal of Climate*, 29(24), 8823–8840. doi: 10.1175/JCLI-D-16-0242.1
- 364 Dong, B., Gregory, J. M., & Sutton, R. T. (2009, jun). Understanding Land–Sea  
 365 Warming Contrast in Response to Increasing Greenhouse Gases. Part I: Transient  
 366 Adjustment. *Journal of Climate*, 22(11), 3079–3097. Retrieved from <https://>

- 367 [journals.ametsoc.org/view/journals/clim/22/11/2009jcli2652.1.xml](https://journals.ametsoc.org/view/journals/clim/22/11/2009jcli2652.1.xml) doi:  
368 10.1175/2009JCLI2652.1
- 369 Dorrington, J., Strommen, K., & Fabiano, F. (2022, apr). Quantifying cli-  
370 mate model representation of the wintertime Euro-Atlantic circulation using  
371 geopotential-jet regimes. *Weather and Climate Dynamics*, 3(2), 505–533. Re-  
372 trieved from <https://wcd.copernicus.org/articles/3/505/2022/> doi:  
373 10.5194/WCD-3-505-2022
- 374 Dorrington, J., & Strommen, K. J. (2020, jun). Jet Speed Variability Obscures  
375 Euro-Atlantic Regime Structure. *Geophysical Research Letters*, 47(15). doi: 10  
376 .1029/2020gl087907
- 377 Driouech, F., Déqué, M., & Sánchez-Gómez, E. (2010, may). Weather  
378 regimes—Moroccan precipitation link in a regional climate change simulation.  
379 *Global and Planetary Change*, 72(1-2), 1–10. doi: 10.1016/J.GLOPLACHA.2010  
380 .03.004
- 381 Fabiano, F., Christensen, H. M., Strommen, K., Athanasiadis, P., Baker, A., Schie-  
382 mann, R., & Corti, S. (2020). Euro-Atlantic weather Regimes in the PRIMAV-  
383 ERA coupled climate simulations: impact of resolution and mean state biases on  
384 model performance. *Climate Dynamics*, 54, 5031–5048. Retrieved from [https://](https://doi.org/10.1007/s00382-020-05271-w)  
385 [doi.org/10.1007/s00382-020-05271-w](https://doi.org/10.1007/s00382-020-05271-w) doi: 10.1007/s00382-020-05271-w
- 386 Fabiano, F., Meccia, V. L., Davini, P., Ghinassi, P., & Corti, S. (2021, mar). A  
387 regime view of future atmospheric circulation changes in northern mid-latitudes.  
388 *Weather and Climate Dynamics*, 2(1), 163–180. doi: 10.5194/wcd-2-163-2021
- 389 Faranda, D., Messori, G., & Yiou, P. (2017, jan). Dynamical proxies of North  
390 Atlantic predictability and extremes. *Scientific Reports 2017 7:1*, 7(1), 1–  
391 10. Retrieved from <https://www.nature.com/articles/srep41278> doi:  
392 10.1038/srep41278
- 393 Ferranti, L., Corti, S., & Janousek, M. (2015, apr). Flow-dependent verifica-  
394 tion of the ECMWF ensemble over the Euro-Atlantic sector. *Quarterly Jour-  
395 nal of the Royal Meteorological Society*, 141(688), 916–924. Retrieved from  
396 <http://doi.wiley.com/10.1002/qj.2411> doi: 10.1002/qj.2411
- 397 Forzieri, G., Feyen, L., Russo, S., Vousdoukas, M., Alfieri, L., Outten, S., ... Cid,  
398 A. (2016, apr). Multi-hazard assessment in Europe under climate change. *Cli-  
399 matic Change*, 137(1-2), 105–119. Retrieved from [https://link.springer.com/](https://link.springer.com/article/10.1007/s10584-016-1661-x)  
400 [article/10.1007/s10584-016-1661-x](https://link.springer.com/article/10.1007/s10584-016-1661-x) doi: 10.1007/s10584-016-1661-x
- 401 Grams, C. M., Beerli, R., Pfenninger, S., Staffell, I., & Wernli, H. (2017, aug).  
402 Balancing Europe’s wind-power output through spatial deployment informed  
403 by weather regimes. *Nature Climate Change*, 7(8), 557–562. doi: 10.1038/  
404 NCLIMATE3338
- 405 Hannachi, A., Woollings, T., & Fraedrich, K. (2012). The North Atlantic jet  
406 stream: A look at preferred positions, paths and transitions. *Quarterly Jour-  
407 nal of the Royal Meteorological Society*, 138(665), 862–877. Retrieved from  
408 <https://rmets.onlinelibrary.wiley.com/doi/pdf/10.1002/qj.959> doi:  
409 10.1002/qj.959
- 410 Joshi, M. M., Gregory, J. M., Webb, M. J., Sexton, D. M., & Johns, T. C. (2008,  
411 apr). Mechanisms for the land/sea warming contrast exhibited by simula-  
412 tions of climate change. *Climate Dynamics*, 30(5), 455–465. Retrieved from  
413 <https://link.springer.com/article/10.1007/s00382-007-0306-1> doi:  
414 10.1007/S00382-007-0306-1/FIGURES/14
- 415 Lorenz, E. N. (1963). Deterministic nonperiodic flow. *Universality in Chaos, Second  
416 Edition*, 20(2), 367–378. doi: 10.1201/9780203734636
- 417 Madonna, E., Li, C., Grams, C. M., & Woollings, T. (2017, oct). The link be-  
418 tween eddy-driven jet variability and weather regimes in the North Atlantic-  
419 European sector. *Quarterly Journal of the Royal Meteorological Society*, 143(708),  
420 2960–2972. Retrieved from <http://doi.wiley.com/10.1002/qj.3155> doi:

- 421 10.1002/qj.3155
- 422 Masato, G., Hoskins, B. J., & Woollings, T. (2013). Winter and Summer Northern  
423 Hemisphere Blocking in CMIP5 Models. *Journal of Climate*, *26*(18), 7044–7059.  
424 doi: 10.1175/JCLI-D-12-00466.1
- 425 Masato, G., Hoskins, B. J., & Woollings, T. J. (2012). Wave-breaking character-  
426 istics of midlatitude blocking. *Quarterly Journal of the Royal Meteorological Soci-  
427 ety*, *138*(666), 1285–1296. Retrieved from [https://rmets.onlinelibrary.wiley](https://rmets.onlinelibrary.wiley.com/doi/pdf/10.1002/qj.990)  
428 [.com/doi/pdf/10.1002/qj.990](https://rmets.onlinelibrary.wiley.com/doi/pdf/10.1002/qj.990) doi: 10.1002/qj.990
- 429 Masato, G., Woollings, T., & Hoskins, B. J. (2014, feb). Structure and im-  
430 pact of atmospheric blocking over the Euro-Atlantic region in present-day and  
431 future simulations. *Geophysical Research Letters*, *41*(3), 1051–1058. doi:  
432 10.1002/2013GL058570
- 433 Michelangeli, P.-A., Vautard, R., Legras, B., Michelangeli, P.-A., Vautard, R.,  
434 & Legras, B. (1995, apr). Weather Regimes: Recurrence and Quasi Sta-  
435 tionarity. *Journal of the Atmospheric Sciences*, *52*(8), 1237–1256. doi:  
436 10.1175/1520-0469(1995)052<1237:WRRAS>2.0.CO;2
- 437 Molteni, F., & Kucharski, F. (2019). A heuristic dynamical model of the North At-  
438 lantic Oscillation with a Lorenz-type chaotic attractor. *Climate Dynamics*, *52*(9-  
439 10), 6173–6193. Retrieved from <https://doi.org/10.1007/s00382-018-4509-4>  
440 doi: 10.1007/s00382-018-4509-4
- 441 Palmer, T. N. (1993, oct). A nonlinear dynamical perspective on climate change.  
442 *Weather*, *48*(10), 314–326. doi: 10.1002/J.1477-8696.1993.TB05802.X
- 443 Palmer, T. N. (1999). A nonlinear dynamical perspective on climate prediction.  
444 *Journal of Climate*, *12*(2), 575–591. doi: 10.1175/1520-0442(1999)012<0575:  
445 ANDPOC>2.0.CO;2
- 446 Parker, T., Woollings, T., Weisheimer, A., O’Reilly, C., Baker, L., & Shaffrey, L.  
447 (2019, aug). Seasonal Predictability of the Winter North Atlantic Oscillation  
448 From a Jet Stream Perspective. *Geophysical Research Letters*, *46*(16), 10159–  
449 10167. Retrieved from [https://onlinelibrary.wiley.com/doi/abs/10.1029/  
450 2019GL084402](https://onlinelibrary.wiley.com/doi/abs/10.1029/2019GL084402) doi: 10.1029/2019GL084402
- 451 Peings, Y., Cattiaux, J., Vavrus, S., & Magnusdottir, G. (2017, aug). Late Twenty-  
452 First-Century Changes in the Midlatitude Atmospheric Circulation in the CESM  
453 Large Ensemble. *Journal of Climate*, *30*(15), 5943–5960. Retrieved from [https://  
454 journals.ametsoc.org/view/journals/clim/30/15/jcli-d-16-0340.1.xml](https://journals.ametsoc.org/view/journals/clim/30/15/jcli-d-16-0340.1.xml)  
455 doi: 10.1175/JCLI-D-16-0340.1
- 456 Rousi, E., Selten, F., Rahmstorf, S., & Coumou, D. (2021, mar). Changes in North  
457 Atlantic Atmospheric Circulation in a Warmer Climate Favor Winter Flood-  
458 ing and Summer Drought over Europe. *Journal of Climate*, *34*(6), 2277–2295.  
459 Retrieved from [https://journals.ametsoc.org/view/journals/clim/34/6/  
460 JCLI-D-20-0311.1.xml](https://journals.ametsoc.org/view/journals/clim/34/6/JCLI-D-20-0311.1.xml) doi: 10.1175/JCLI-D-20-0311.1
- 461 Schiemann, R., Athanasiadis, P., Barriopedro, D., Doblas-Reyes, F., Lohmann, K.,  
462 Roberts, M. J., ... Vidale, P. L. (2020, jun). Northern Hemisphere blocking  
463 simulation in current climate models: evaluating progress from the Climate Model  
464 Intercomparison Project Phase 5 to 6 and sensitivity to resolution. *Weather and  
465 Climate Dynamics*, *1*(1), 277–292. doi: 10.5194/WCD-1-277-2020
- 466 Shepherd, T. G. (2014, sep). Atmospheric circulation as a source of uncertainty in  
467 climate change projections. *Nature Geoscience*, *7*(10), 703–708. Retrieved from  
468 <https://www.nature.com/articles/ngeo2253> doi: 10.1038/NCEO2253
- 469 Shepherd, T. G. (2019, may). Storyline approach to the construction of regional  
470 climate change information. *Proceedings of the Royal Society A*, *475*(2225).  
471 Retrieved from [https://royalsocietypublishing.org/doi/full/10.1098/  
472 rspa.2019.0013](https://royalsocietypublishing.org/doi/full/10.1098/rspa.2019.0013) doi: 10.1098/RSPA.2019.0013
- 473 Smith, D. M., Scaife, A. A., Eade, R., Athanasiadis, P., Bellucci, A., Bethke, I.,  
474 ... Zhang, L. (2020, jul). North Atlantic climate far more predictable than

- 475 models imply. *Nature* 2020 583:7818, 583(7818), 796–800. Retrieved from  
476 <https://www.nature.com/articles/s41586-020-2525-0> doi: 10.1038/  
477 s41586-020-2525-0
- 478 Vallis, G. K., Zurita-Gotor, P., Cairns, C., & Kidston, J. (2015, jul). Response of  
479 the large-scale structure of the atmosphere to global warming. *Quarterly Journal*  
480 *of the Royal Meteorological Society*, 141(690), 1479–1501. doi: 10.1002/QJ.2456
- 481 van der Wiel, K., Bloomfield, H. C., Lee, R. W., Stoop, L. P., Blackport, R., Screen,  
482 J. A., & Selten, F. M. (2019, sep). The influence of weather regimes on European  
483 renewable energy production and demand. *Environmental Research Letters*, 14(9),  
484 094010. doi: 10.1088/1748-9326/ab38d3
- 485 Weisheimer, A., Schaller, N., O’Reilly, C., MacLeod, D. A., & Palmer, T. (2017).  
486 Atmospheric seasonal forecasts of the twentieth century: multi-decadal variabil-  
487 ity in predictive skill of the winter North Atlantic Oscillation (NAO) and their  
488 potential value for extreme event attribution. *Quarterly Journal of the Royal Me-*  
489 *teorological Society*, 143(703), 917–926. Retrieved from [http://doi.wiley.com/](http://doi.wiley.com/10.1002/qj.2976)  
490 [10.1002/qj.2976](http://doi.wiley.com/10.1002/qj.2976) doi: 10.1002/qj.2976
- 491 Woollings, T., Hannachi, A., & Hoskins, B. (2010, may). Variability of the North  
492 Atlantic eddy-driven jet stream. *Quarterly Journal of the Royal Meteorological*  
493 *Society*, 136(649), 856–868. Retrieved from [http://doi.wiley.com/10.1002/](http://doi.wiley.com/10.1002/qj.625)  
494 [qj.625](http://doi.wiley.com/10.1002/qj.625) doi: 10.1002/qj.625
- 495 Woollings, T. J., Hoskins, B., Blackburn, M., & Berrisford, P. (2008, feb). A new  
496 Rossby wave-breaking interpretation of the North Atlantic Oscillation. *Journal of*  
497 *the Atmospheric Sciences*, 65(2), 609–626. doi: 10.1175/2007JAS2347.1
- 498 Zappa, G., & Shepherd, T. G. (2017, aug). Storylines of Atmospheric Circulation  
499 Change for European Regional Climate Impact Assessment. *Journal of Climate*,  
500 30(16), 6561–6577. Retrieved from [https://journals.ametsoc.org/view/](https://journals.ametsoc.org/view/journals/clim/30/16/jcli-d-16-0807.1.xml)  
501 [journals/clim/30/16/jcli-d-16-0807.1.xml](https://journals.ametsoc.org/view/journals/clim/30/16/jcli-d-16-0807.1.xml) doi: 10.1175/JCLI-D-16-0807.1

# Supporting information for "Wintertime blocking regimes over Europe are projected to become less persistent in a warming climate"

Josh Dorrington<sup>1,2</sup>, Kristian Strommen<sup>1</sup>, Federico Fabiano<sup>3</sup>, Franco Molteni<sup>4</sup>

<sup>[1]</sup>

]Atmospheric, Oceanic, and Planetary Physics, University of Oxford, Oxford, UK

<sup>[2]</sup>

]Institute for Meteorology and Climate (IMK-TRO), Karlsruher Institute of Technology, Germany

<sup>[3]</sup>

]Institute of Atmospheric Sciences and Climate (ISAC-CNR), Bologna, Italy

<sup>4</sup>European Centre for Medium Range Weather Forecasting, Shinfield Road, Reading, UK

---

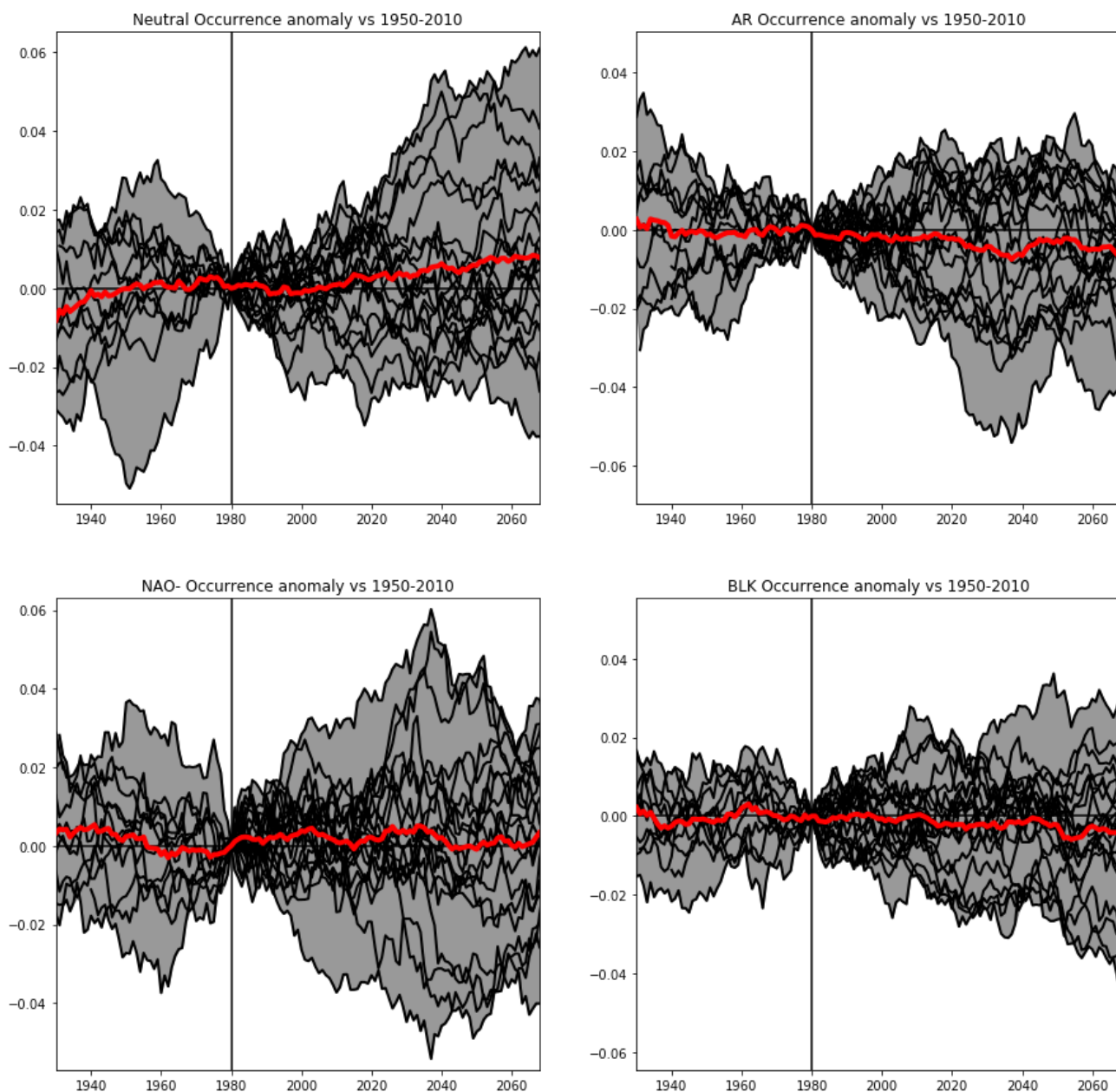


**Figure S1.** Sixty year rolling windows of regime occurrence, with each CMIP6 model shown in black, and with the ensemble mean (as shown in the left panel of main figure 2) in red. The vertical line marks the reference period of 1950-2010. Shading captures the full range of intermodel spread.

Model name	Ensemble member
ACCESS-CM2	r1i1p1f1
BCC-CSM2	r1i1p1f1
CanESM5	r1i1p1f1
CNRM-CM6-1	r1i1p1f2
CNRM-CM6-1-HR	r1i1p1f2
CNRM-ESM2	r1i1p1f2
EC-Earth3	r1i1p1f1
FGOALS-g3	r1i1p1f1
GFDL-CM4	r1i1p1f1
HadGEM3-GC31-LL	r1i1p1f3
HadGEM3-GC31-MM	r1i1p1f3
INM-CM4-8	r1i1p1f1
INM-CM5-0	r1i1p1f1
IPSL-CM6A-LR	r1i1p1f1
MIROC6	r1i1p1f1
MPI-ESM1-2-HR	r1i1p1f1
MPI-ESM1-2-LR	r1i1p1f1
MRI-ESM2-0	r1i1p1f1
NorESM2-LM	r1i1p1f1
NorESM2-MM	r1i1p1f1
UKESM1-0-LL	r1i1p1f2

**Table S1.** CMIP6 models whose simulations were used, for both historical and SSP58.5.